Workspace and singularity analysis of 3-RRR planar parallel manipulator

Ketankumar H Patel
Department of Mechanical Engineering
A D Patel Institute of Technology
New Vallabh Vidyanagar, Gujarat, India
khpatel1990@yahoo.com

Vinit C Nayakpara
Department of Mechanical Engineering
A D Patel Institute of Technology
New Vallabh Vidyanagar, Gujarat, India
nayakpara.vinit3@gmail.com

Yogin K Patel
Department of Mechanical Engineering
A D Patel Institute of Technology
New Vallabh Vidyanagar, Gujarat, India
yogin.patel23@gmail.com

Y D Patel
Department of Mechanical Engineering
A D Patel Institute of Technology
New Vallabh Vidyanagar, Gujarat, India
yash523@rediffmail.com

***Abstract*—Nowadays, Planar Parallel Manipulators (PPMs) are widely used due to many inherent characteristics over the serial manipulator. In this paper, PPM with 3-RRR (revolute joints) configuration is simulated using Pro/mechanism and investigated analytically. Revolute joints are considered as joints with virtually no mechanical limits so that the workspace can be maximized. Loop closure equations are formulated for the 3-RRR manipulator and Jacobian matrices are developed for singularity analysis. For the proposed mechanism, singularity analysis is carried out using Instantaneous Center of Rotation (ICR) method. With regard to planar parallel manipulators, singularity can be classified into three groups based on properties of instantaneous center of rotation. This method is very fast and can easily be applied to the manipulators under study. The results of ICR are compared using analytical approach. Functional workspace of planar parallel manipulator is developed by actuating different combination of servomotors and is often limited because of interference among their mechanical components.**

Keywords—Planar Parallel Manipulator (PPM), Instantaneous center of rotation (ICR), Jacobian, Workspace, Singularity.

I. INTRODUCTION

A Parallel manipulator can be defined as a closed loop mechanism composed of an end-effector and a fixed base, linked together by at least two independent kinematic chains. A serial manipulator referred as open-loop manipulator because it's one end connected to ground and other end is free to move in space. Significance of parallel manipulator over serial manipulator is its higher payload-to-weight ratio, high accuracy, high structural rigidity and low inertia of moving parts [1]. Many industrial and non-industrial applications of parallel manipulators include automobile organizations, medical and space science, military artilleries, food and beverage, ship building, construction, aircraft and aerospace organizations. Researchers have focused their work for spatial parallel manipulators but usage of such planar configurations may not be neglected. There are seven different types of planar parallel manipulator (PPM) RPP, RRP, RRR, RPR, PRR, PRP and PPR as reported in [2, 3]. Singularity loci of 3-DOF planar parallel manipulator are presented by Ilian A. Bonev and Cl´ement M. Gosselin [4]. Different types of singularities are explained for 3-RRR and 3-RPR configurations along with kinematic description as well as its analysis by Clement Gosselin [5]. In opposite to serial manipulators, parallel manipulators can admit not only multiple inverse kinematic solutions, but also multiple direct kinematic solutions. This property produces more complicated kinematic models but allows more flexibility in trajectory planning [6]. Serdar Kucuk explained particle swarm optimization problem for the 3 degrees of freedom RRR fully planar parallel manipulator (3-RRR) for less energy requirements and improved performance of the manipulator [7]. Singularities are classified with interpretation and instantaneous centre method is proposed for all planar parallel manipulators to understand their singularities [8]. Significance of 3-RRR PPM over other configurations is ease in assembly, operational and control aspects. Various applications of such 3-RRR planar parallel configurations are pick and place operation over a plane surface, machining of plane surfaces, mobile base for a spatial manipulator and moving platform for a terrestrial vehicle simulator as discussed. In the present study, the simulation study provides further insight into the potentials of the 3-RRR robotic manipulator for various functions generation within workspace for the given operating conditions and control. This paper has limited scope up to kinematic analysis, singularity and simulation of workspace generation using pro/engineer software.

II. MOBILITY ANALYSIS AND MODELING OF 3-RRR PPM

3-RRR PPM is considered for its study, which consists of one platform, six linkages, one tripod (end effector) with tool mounted at the center and actuated by three servomotors. The actuators are fixed to the base allows the use of inexpensive DC drives and reduces the weight and

power requirements of the mobile equipment. The manipulator is modeled using Pro/Mechanism constraints as shown in fig. 1. Links connected to servo motors are active while the remaining are passive links connected with moving platform.

Degrees of freedom (DOF) are the set of independent displacements and/or rotations that specify completely the displaced or deformed position and orientation of the body or system. The degree of freedom (DOF) for planar configuration as shown in fig. 1 is computed using Gruebler's equation as,

$$DOF = 3(N-1) - 2J_1 - J_2 \quad (1)$$
$$= 3(8-1) - 2(9) = 3$$

Where, N = Number of links. , J_1 = Number of revolute joint with one DOF, J_2 = Number of joint with two DOF. Number of limbs in parallel manipulator are same as number of degree of freedom.

Using Euler's equation, number of independent loops (l), joints (j) and links(N) of a mechanism are related by,

$$l = J - N + 1 = 9 - 8 + 1 = 2$$

In the 3-RRR Mechanism, there are 9 revolute joints and 8 links (6 links+1 moving platform+ 1 fixed base). The configuration is fully parallel manipulator as each limb has only one actuator. Three servo motors are attached at $M_1, M_2$and M_3 locations as active joints. The remaining six revolute joints act as passive joints.

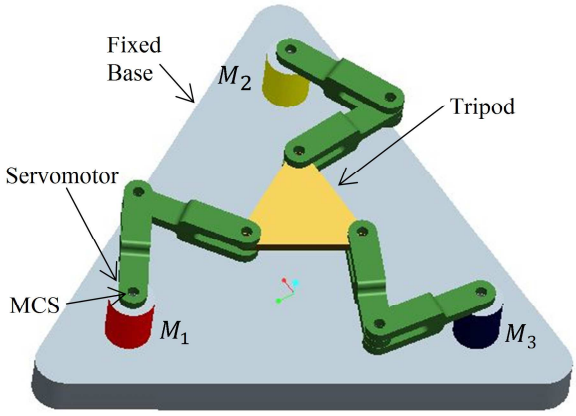

Fig. 1 Architecture of 3-RRR planar parallel manipulator

III. FORMULATION OF LOOP CLOSURE EQUATIONS

In the present work, relationship between different variables can be obtained with the help of loop closure equations. Loop closure equations are obtained by taking projection of links on X-axis and Y-axis forming a closed loop. In parallel manipulators, there are single or multiple loops but nothing likes a first or last loop in formulation of loop closure equations. In above configuration, three closed loops are formed between three active joints. Three loops are formed between servo-motors M_1 and M_3, M_3 and M_2, and M_2 and M_1 as shown in fig. 2

The resulting equations are,

$$l_1 \cos\theta_1 + r_1 \cos\phi_1 + a\cos\alpha - r_3 \cos\phi_3 - l_3 \cos\theta_3 - x_3 = 0$$
$$l_1 \sin\theta_1 + r_1 \sin\phi_1 + a\sin\alpha - r_3 \sin\phi_3 - l_3 \sin\theta_3 = 0 \quad (2a)$$
$$x_3 + l_3 \cos\theta_3 + r_3 \cos\phi_3 + a\cos(2\pi/3 + \alpha) - r_2 \cos\phi_2 - l_2 \cos\theta_2 - x_2 = 0$$
$$l_3 \sin\theta_3 + r_3 \sin\phi_3 + a\sin(2\pi/3 + \alpha) - r_2 \sin\phi_2 - l_2 \sin\theta_2 - y_2 = 0 \quad (2b)$$
$$l_1 \cos\theta_1 + r_1 \cos\phi_1 + a\cos(\pi/3 + \alpha) - r_2 \cos\phi_2 - l_2 \cos\theta_2 - x_2 = 0$$
$$l_1 \sin\theta_1 + r_1 \sin\phi_1 + a\sin(\pi/3 + \alpha) - r_2 \sin\phi_2 - l_2 \sin\theta_2 - y_2 = 0 \quad (2c)$$

Where, l_i=length of active links, i=1, 2, 3
r_i=length of passive links
a=side of tripod.

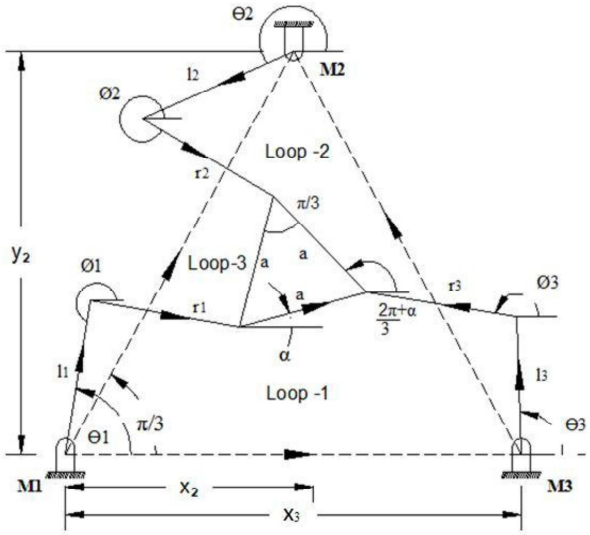

Fig. 2 Planar 3-RRR manipulator

IV. SIMULATION IN PRO/ENGINEER

Simulation of the manipulator is carried out using Pro/Engineer software to compare the analytical results of kinematics, joints range determination and workspace generation. The model of 3-RRR planar manipulator is developed using mechanism constraints. Fixed platform provides base for manipulator. Active and passive links transform motion to the end effector. Tripod is an equilateral triangle with side "a" and tool mounted on its centroid. All the parts are assembled with the help of axis alignment and surface alignment constraints as shown in fig. 1. For this assembly pin joints are used. Model Coordinate System (MCS) is placed at location M_1. All servo-motors are constant velocity type with constant magnitude of angular velocity 6° per second. The following dimensions are chosen for investigation of manipulator under consideration. Distance between two servo-motors is $|M_1M_2| = |M_2M_3| = |M_1M_3| = 300$ mm. Length of each link (l, r) is 100 mm. Each side of tripod is 100 mm. Initially, kinematic analysis is simulated with arbitrary

time. Using collision detection option as shown in fig. 3, the actual time for simulation is determined.

Three different types of collision detection features are available in the software. No collision detection feature does not detect any collision and enables a smooth dragging even in case of collision. Partial collision detection feature specifies the parts between which to check for collision. Global collision detection feature checks for any kind of collision in the entire assembly and indicates it according to the option chosen. In the simulation of 3-RRR manipulator, global collision detection feature available is utilized and the joint ranges of servo motors are determined based on individual measure of angular position with respect to reference position at time of collision. The assumed initial positions for link1, 2 and 3 are shown in table-I and tripod centre coordinates are (150, 86.5959). Angle α represents tripod orientation as shown in fig. 2 is assumed parallel to X-axis initially and its value is zero.

TABLE I ASSUMED INITIAL POSITIONS FOR MODEL

Active Variable	Initial	Passive Variable	Initial
θ_1	84.73°	ϕ_1	-24.74
θ_2	-35.27°	ϕ_2	-144.74
θ_3	-155.26°	ϕ_3	95.25

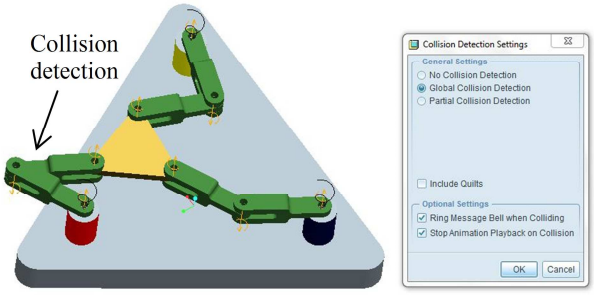

Fig. 3 Global collision detection in 3-RRR PPM

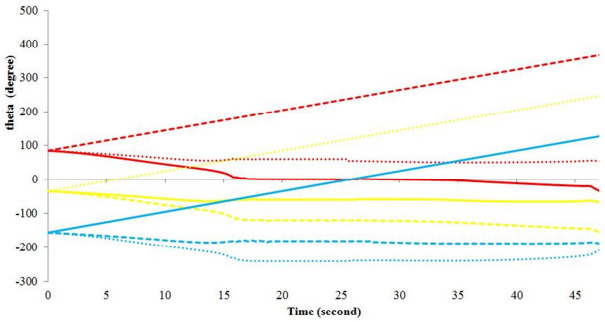

Fig. 4(a) Collision between links when actuated individually in counter-clockwise direction

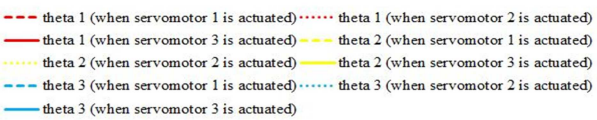

It is observed that existence of entirely linear curve only for the single actuated joint but linearity is lost after some portion of the curve for two remaining un-actuated limb because of volumetric interference of rigid bodies of the mechanism. The non linear behavior shows the collision among the links due to over traverse of the remaining active joints.

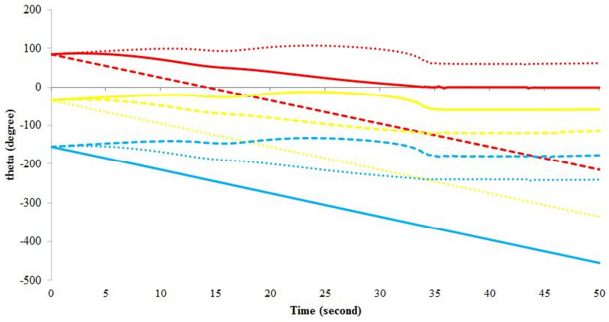

Fig. 4(b) Collision between links when actuated individually in clockwise direction

The figures 4(a) and 4(b) show linear and non-linear part of the curve at time of a single joint actuation either M_1, M_2 or M_3. The initiation of non linear behavior of the curve corresponds to single actuation indicates the limits of joint range for that active joint for counter clockwise and clockwise motion of active servo motor.

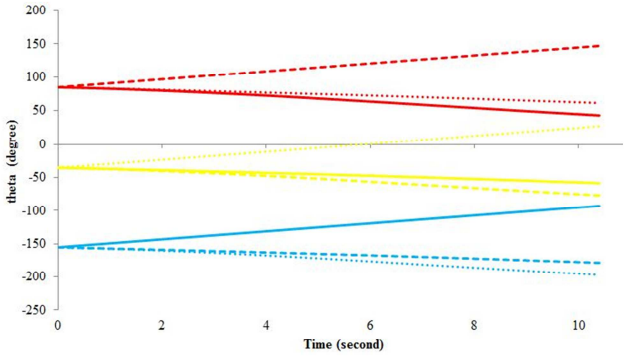

Fig. 5(a) Graph showing joint range of servomotors when actuated individually in counter-clockwise direction

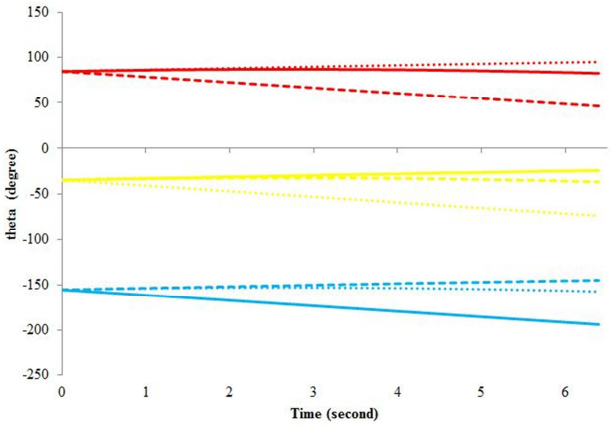

Fig. 5(b) Graph showing joint range of servomotors when actuated individually in clockwise direction

Using global collision detection, any volumetric interference among any moving or stationary component of the assembly leads to end of the mechanism simulation

automatically. Figures 5(a) and 5(b) are obtained directly by the software using global collision detection feature. This helps in determination of working range of the active joints under consideration. The range of the active and passive joint variables for different analysis is tabulated as shown in table II.

TABLE II ALLOWABLE RANGE OF MOTION FOR JOINT VARIABLES

Analysis	End Time	$\theta_1, \theta_2, \theta_3$ (degree)	ϕ_1, ϕ_2, ϕ_3 (degree)	α (degree)
Initial position	0s	84.7290	-24.7346	0.0000
		-35.2656	-144.7349	
		-155.2601	95.2485	
range1 (ccw)	10.4s	147.1310	3.8388	-6.0791
		-76.9712	-168.1173	
		-178.4993	-211.9887	
range2 (ccw)	10.4s	61.4898	28.0062	-6.0791
		27.1296	-116.1557	
		-196.9772	163.0180	
range3 (ccw)	10.4s	43.0177	-48.1170	-6.0791
		-58.5047	-88.0120	
		-92.8593	-236.1503	
range1 (cw)	6.4s	46.3294	-34.2514	12.3702
		-37.2365	-118.4361	
		-144.8666	71.8374	
range2 (cw)	6.4s	95.1396	-48.1628	12.3472
		-73.6652	-154.2402	
		-157.2196	-238.4135	
range3 (cw)	6.4s	82.7408	1.5011	12.4217
		-24.9409	-168.1803	
		-193.6597	85.7317	

The change of angle from assumed initial position is reflected in table III for counter clockwise and clockwise rotation of each servo motor.

TABLE III ALLOWABLE CHANGE IN ANGLE FROM ASSUMED INITIAL POSITION

Servo-motor	Direction of rotation	End time	Change in angle from assumed initial position
M_1	Counter clock wise	10.4s	62.4^o
M_1	Clock wise	6.4s	38.4^o
M_2	Counter clock wise	10.4s	62.4^o
M_2	Clock wise	6.4s	38.4^o
M_3	Counter clock wise	10.4s	62.4^o
M_3	Clock wise	6.4s	38.4^o

When individual servo motor is actuated, then the entire range of servo-motor is as follows:

TABLE IV JOINT RANGE OF SERVO-MOTOR

Servo-motor	**Joint Range of servo-motor**		**Total Joint Range**
	Counter clock wise	**Clock wise**	
	from assumed initial position		
M_1	62.4^o	38.4^o	100.8^o
M_2	62.4^o	38.4^o	100.8^o
M_3	62.4^o	38.4^o	100.8^o

The entire procedure for determination of joint ranges for active joints using global collision detection method is summarized as shown in fig. 6.

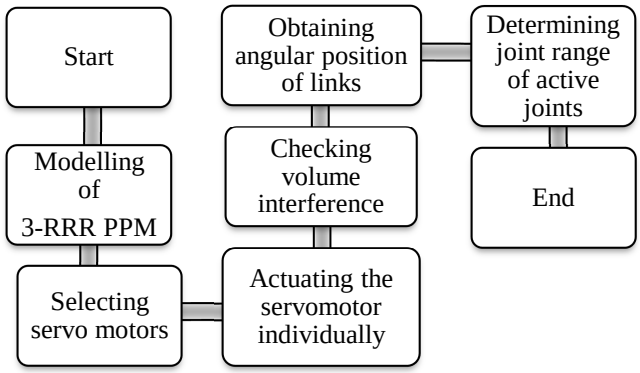

Fig. 6 Summary of modeling and simulation in Pro/E

V. SINGULARITY ANALYSIS

Algebraically, singularity is a result of a rank deficiency of the Jacobian matrices; geometrically, singularity is observed whenever the manipulator gains some additional, uncontrollable degrees of freedom (DOF), or loses some DOF. Similarly, the force transmission performance of a parallel manipulator is very poor near singular configurations as reported in [8].

A. Analytical method

By differentiating loop closure equations (2a) to (2c) with respect to $\theta_i = \{\theta_1, \theta_2, \theta_3\}$ and $\phi_i = \{\phi_1, \phi_2, \phi_3, \alpha\}^T$

$$[J]_\theta \dot{\theta} + [J]_\phi \dot{\phi} = 0 \tag{3}$$

Where,

$$[J]_\theta = \begin{bmatrix} -l_1 \sin\theta_1 & 0 & l_3 \sin\theta_3 \\ l_1 \cos\theta_1 & 0 & -l_3 \cos\theta_3 \\ 0 & l_2 \sin\theta_2 & -l_3 \sin\theta_3 \end{bmatrix} \tag{4}$$

$$[J]_\phi = \begin{bmatrix} -r_1 \sin\phi_1 & 0 & r_3 \sin\phi_3 & -a \sin\alpha \\ r_1 \cos\phi_1 & 0 & -r_3 \cos\phi_3 & a \cos\alpha \\ 0 & r_2 \sin\phi_2 & -r_3 \sin\phi_3 & -a \sin\left(\frac{2\pi}{3}+\alpha\right) \\ 0 & -r_2 \cos\phi_2 & r_3 \cos\phi_3 & a \cos\left(\frac{2\pi}{3}+\alpha\right) \end{bmatrix} \tag{5}$$

The criterion to determine the singularity is

$$\det[J]_\theta = 0 \tag{6a}$$

$$[\cos(\theta_1)\sin(\theta_2)\sin(\theta_3) - \sin(\theta_1)\sin(\theta_2)\cos(\theta_3)] = 0$$

$$\det[J]_\phi = 0 \tag{6b}$$

$$\left[\sin\left(\frac{2\pi}{3}+\alpha-\phi_2\right)\sin(\phi_1-\phi_3) + \sin(\phi_3-\phi_2)\sin(\phi_1-\alpha)\right] = 0$$

B. Instantaneous Center of Rotation (ICR)

The instantaneous center of rotation (ICR) is defined as the instantaneous location of a pair of coincident points of two rigid bodies, the absolute velocities of which are equal. In the other words, one rigid body can rotate about the ICR, relative to the other one. The ICR is defined between any two rigid bodies that have relative planar

motion. Therefore, there are three ICRs between three rigid bodies with relative motion. They are related by the following well known theorems. According to Arnhold–Kennedy theorem three instant centers of rotation shared by three rigid bodies in relative motion to one another all lie on the same line and there is no relative motion between two rigid bodies in the absence of any ICR between them [8]. In serial manipulators, singularities occur whenever one actuator does not produce any motion of the end effector. In parallel manipulators, in addition to the foregoing, there exists another type of singularity, in which the end effector cannot resist forces or torques in one or more directions, even if all the actuators are locked. Thus, one can classify singularities into three groups [8]. First, second and third types of singularities are represented in fig. 7, 8 and 9 respectively.

The first type of singularity

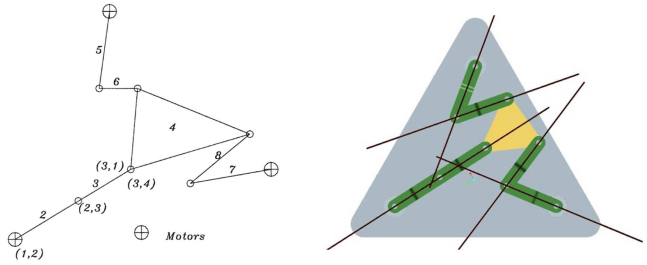

Fig. 7(a) Example of the first type of singularity in which one leg is fully extended [8]

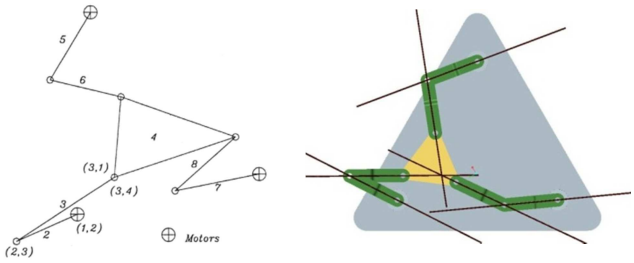

Fig. 7(b) Example of the first type of singularity in which one leg is folded [8]

In this case, the manipulator may loose one degree of freedom and configuration requires excessive amount of force for its movement or links may be structurally deflected if it is operated in this nearby areas. Ultimately, there will be loss of accuracy due to this structural deflection permanently as shown in fig. 7.

The second type of singularity

In second type of singularity, the configuration may gain one degree of freedom as shown in fig. 8(a) and 8(b). In third type of singularity also the mechanism may be locked sometimes. Hence, the singularity regions must be avoided as far as good performance of manipulator is concerned. The existence of third type of singularities will be only when the first and second type of singularities are existing simultaneously.

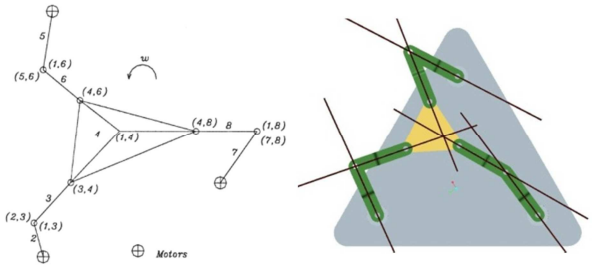

Fig. 8(a) Second type of singularity with links intersect at a point [8]

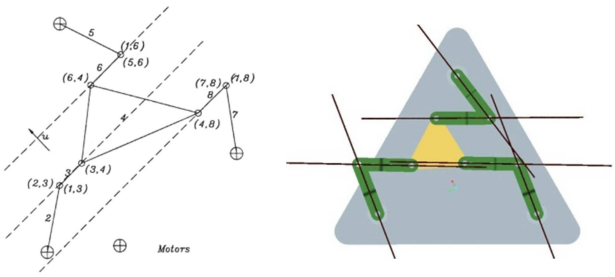

Fig. 8(b) Second type of singularity with links are parallel [8]

The third type of singularity

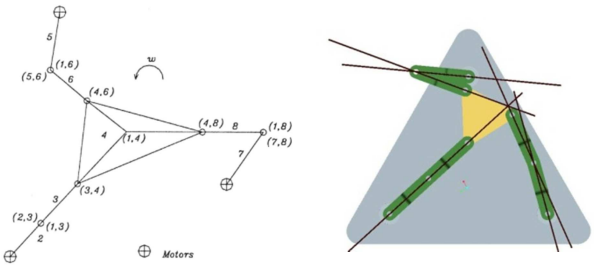

Fig. 9(a) Third type of singularity with one leg fully extended and passive links intersect at a point [8]

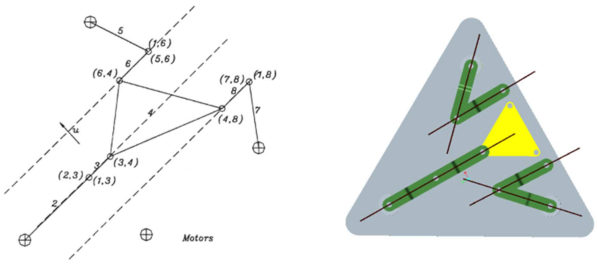

Fig. 9(b) Third type of singularity with one leg fully extended and passive links are parallel to each other [8]

By substituting the value $\theta_1, \theta_2, \theta_3, \phi_1, \phi_2, \phi_3$ *and* α in equation (6a) and (6b) for different types of singularity, one can find $\det[J]_\theta$ and $\det[J]_\phi$ which is tabulated in table V.

From table V, one can conclude that for any type of singularity (first, second or third), the value of $\det[J]_\theta$ and $\det[J]_\phi$ is nearer to zero. There is existence of boundary and interior singularity in this 3-RRR manipulator configuration.

TABLE V JOINT RANGE OF SERVO-MOTOR

Type	Sub classification	$\theta_1, \theta_2, \theta_3$ Degree	$\phi_1, \phi_2, \phi_3, \alpha$ Degree	$\det[J]_\theta$ $\det[J]_\phi$
1	Fully extended	32.687, 249.39, 157.43	32.687, 19.319, 53.029, 5.8897	-0.76, -0.08
	Fully folded	152.97, 200.61, 185.39	0.3923, 278.648, 154.581, 352.75	-0.18, -0.003
2	Passive links Intersect at a point	114.41, 152.52, 126.89	18.977, 291.587, 150.364, 3.3563	0.09, -0.01
	Passive links are parallel	110.92, 307.34, 111.00	358.73, 180.306, 178.886, 2.3511	-0.001, -0.0006
3	Fully extended and intersect at a point	42.319, 174.51, 105.42	42.319, 339.648, 114.069, 32.119	0.08, 0.002
	Fully extended and Links are parallel	30, 254, 162	30, 30, 30, 0	-0.71, 0

Type 1 singularity is normally represents boundary singularity when the legs are fully extended or folded. Type 2 singularity is a case of interior singularity. Type 3 singularity is again a case of boundary singularity.

VI. WORKSPACE DETERMINATION USING SIMULATION (PRO/E)

Workspace is defined as a volume of space which the end-effector of the manipulator can reach.

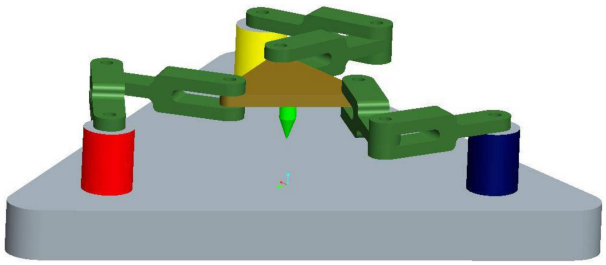

Fig. 10 Tool mounted at the tripod center

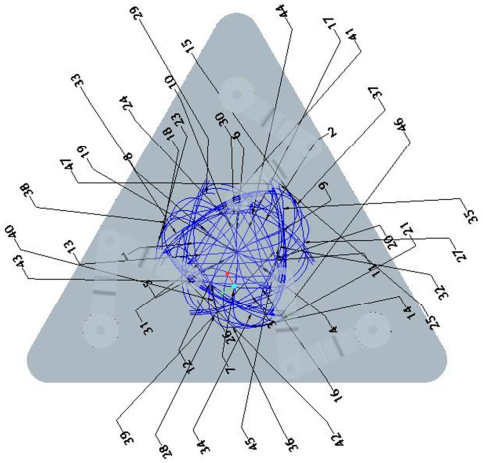

Fig. 11 Workspace generated for various combination

The workspace determination of parallel manipulators is one of the most important issues especially in measuring its suitability for a conceptual kinematic design. The point cloud of tool tip coordinates as shown in fig. 10 is used for workspace development of 3-RRR planar parallel manipulator.

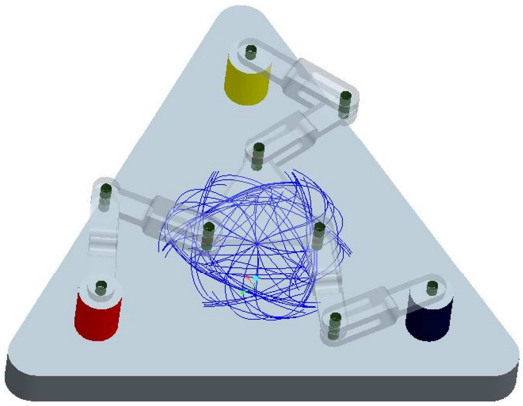

Fig.12 Workspace generated using various combinations of servomotors

Functional workspace of planar parallel manipulator is often limited because of interference among their mechanical components. Workspace of 3-RRR manipulator is obtained by actuating different combination of servo motors as shown in fig. 11, using global collision detection and providing time lag between different servomotors and is shown in fig.12.

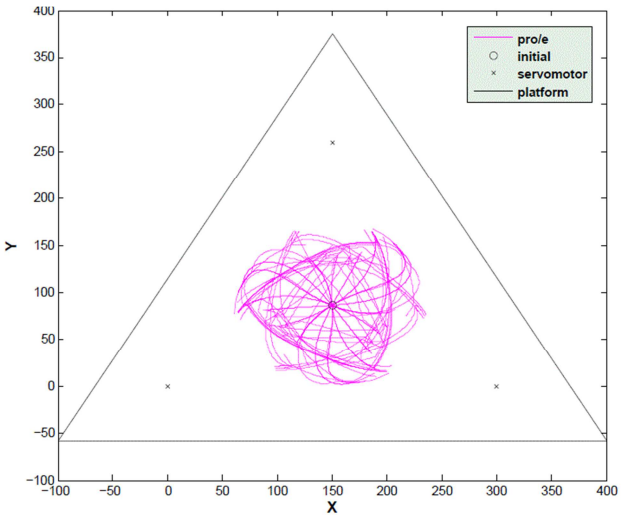

Fig.13 Workspace generated using various combinations of servomotors

Above Fig.13 shows workspace generated using Pro/E of 3-RRR manipulator. In above graph the legend Pro/E represents workspace obtained using Pro/E, initial means regenerate position of tripod, servomotor represents positions of three servomotors and platform represents the base of the manipulator. One can increase the region of Pro/E workspace by changing links dimensions. More combinations of servo motors with different time lag will further improve actual workspace.

TABLE VI MAXIMUM AND MINIMUM VALUE OF DIFFERENT VARIABLES

Variable Value*	Initial	Minimum	Maximum
Theta 1 (θ_1)	84.73	-94.47545144	153.6490636
Theta 2 (θ_2)	-35.27	-214.1763508	33.64598771
Theta 3 (θ_3)	-155.26	-334.1952915	-86.34958764
Phi 1 (ϕ_1)	-24.74	-82.16855647	89.98284832
Phi 2 (ϕ_2)	-144.74	157.8214904	269.9860696
Phi 3 (ϕ_3)	95.25	90.00086998	226.736788
Alpha (α)	0	-298.8968273	59.92573407
X- coordinate of Tripod center (mm)	150	60.87284048	235.8237586
Y- coordinate of Tripod center (mm)	86.5959	2.222825524	167.8777484

$*\ \theta_1, \theta_2, \theta_3, \phi_1, \phi_2, \phi_3$, α are in degree.

Table VI represents variations of active and passive joint variables for their extreme limits through simulation using software. Figure 14 shows the sequence of operations to be performed for simulation of work space generation using software.

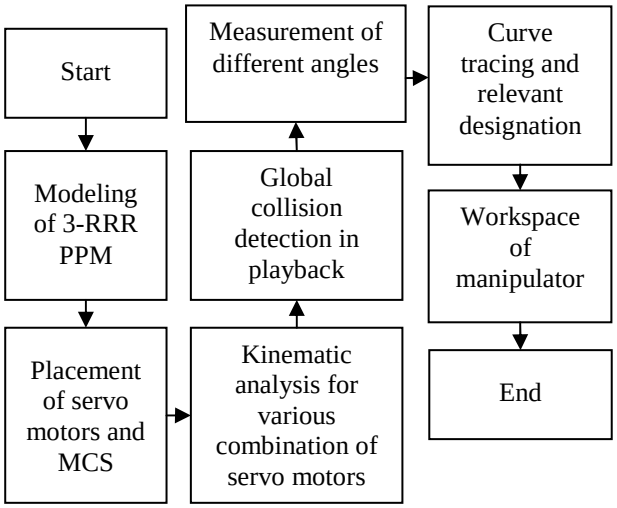

Fig.14 Process flow chart to obtain workspace in Pro/E

VII. CONCLUSION

Forward kinematic and singularity analysis of 3-RRR planar parallel manipulator is investigated. Collision detection method in Pro/Engineer is advantageous, faster and has better visualization compared to analytic kinematic real time simulation using matlab. The assumed initial position of configuration under consideration is axi-symmetric, the corresponding joint range obtained for all three servo-motors is same (i.e. Joint range=100.8°) as per table IV. Based on assumed initial position of the configuration, the joint range may vary. It is observed that for any type of singularity (first, second or third), the value of $\det[J]_\theta$ and $\det[J]_\phi$is nearer to zero as shown in table V. Different cases of singularity configurations are illustrated. Type 1 and type 3 singularity are typical cases of boundary singularities. Type 2 is a special case of interior singularity. Using systematic manipulation of point clouds obtained after kinematic analysis, workspace is generated using Pro/E as shown in fig. 13. Workspace as well as performance of the manipulator can be further improved by changing dimensions of linkages or modifying shape of the link.

REFERENCES

[1] Balan R., V. Maties, S. Stan, C. Lapusan, On the Control of a 3-RRR Planar Parallel Minirobot, Journal *Mecatronica*, Journal of Romanian Society of Mechatronics, no. 4/2005, ISSN 1583-7653, pp. 20-23, December, 2005.

[2] A. K. Dash, I. -M. Chen, S. H. Yeo, G. Yang, "Task-oriented configuration design for reconfigurable parallel manipulator systems", International Journal of Computer Integrated Manufacturing, Vol. 18, No. 7, pp. 615-634, 2005

[3] Serdar Kucuk, "A dexterity comparison for 3-DOF planar parallel manipulators with two kinematic chains using genetic algorithms", Mechatronics, Vol. 19, No.6, pp. 868‑877, 2009.

[4] Bonev I.A. and Gosselin C.M. Singularity Loci of Planar Parallel Manipulators with Revolute Joints. In F.C. Park C.C. Iurascu, editor, *Computational Kinematics*, Seoul, South Korea, pages 291–299, May 2001.

[5] Clement Gosselin, "Kinematic analysis, optimization and programming of parallel robotic manipulator", Ph.D Thesis, Department of mechanical engineering, McGill University, Montreal, Canada, pp. 83-91, June 1988.

[6] Damien Chablat, Philippe Wenger, "The Kinematic Analysis of a Symmetrical Three-Degree-of-Freedom Planar Parallel Manipulator", CoRR abs/0705.0959, France, pp. 1-8, 2007

[7] SerdarKucuk – "Energy minimization for 3-RRR fully planar parallel manipulator using particle swarm optimization", Department of Biomedical Engineering, Kocaeli University, 41380, Izmit, Turkey, pp. 129-149, November 2012.

[8] H. R. Mohammadi Daniali, "Instantaneous center of rotation and singularities of planar parallel manipulators", Int. J. of Mech. Eng. Education, Vol. 33, No. 3, pp. 251-259, 2005

[9] C. Nasa and S. Bandyopadhyay, "Trajectory-tracking control of a planar 3-RRR parallel manipulator with singularity avoidance", Robotics and Mechatronics, 13th World Congress in Mechanism and Machine Science, Robotics and Mechatronics, Mexico, pp. 19-25, June 2011.